# Long-term immune protection against SARS-CoV-2 escape variants upon a single vaccination with murine cytomegalovirus expressing the spike protein

Yeonsu Kim[1], Henning Jacobsen[1], Bettina Fuerholzner[1], Kathrin Eschke[1], Markus Hoffmann[2,3,], M.Zeeshan Chaudhry[1], Federico Bertoglio[4], Michael Hust[4], Marek Widera[5], Sandra Ciesek[5,6,7], Stefan Pöhlmann[2,3], Luka Čičin-Šain[1, 8,9, *]

1. Department of Viral Immunology, Helmholtz Centre for Infection Research (HZI), Braunschweig, Germany

2. Infection Biology Unit, German Primate Center, Göttingen, Germany

3. Faculty of Biology and Psychology, Georg-August-University Göttingen, Göttingen, Germany

4. Department of Medical Biotechnology, Institute for Biochemistry, Biotechnology and Bioinformatics, Technical University Braunschweig, Braunschweig, Germany

5. Institute for Medical Virology, University Hospital Frankfurt, Goethe University Frankfurt, Frankfurt am Main, Germany

6. Fraunhofer Institute for Translational Medicine and Pharmacology ITMP, Frankfurt am Main, Germany

7. German Centre for Infection Research (DZIF), External partner site Frankfurt, Germany

8. German Centre for Infection Research (DZIF), Hannover-Braunschweig Site, Germany

9. Centre for Individualized Infection medicine (CiiM), a joint venture of HZI and MHH, Hannover, Germany

*. Correspondence: Luka.Cicin-Sain@helmholtz-hzi.de

## Abstract

**Vaccines are central to controlling the coronavirus disease 2019 (COVID-19) pandemic but the durability of protection is limited for currently approved COVID-19 vaccines. Further, the emergence of variants of concern (VoCs) that evade immune recognition has reduced vaccine effectiveness, compounding the problem. Here, we show that a single dose of a murine cytomegalovirus (MCMV)-based vaccine, which expresses the spike (S) protein of the virus circulating early in the pandemic (MCMV$^S$), protects highly susceptible K18-hACE2 mice from clinical symptoms and death upon challenge with a lethal dose of D614G SARS-CoV-2. Moreover, MCMV$^S$ vaccination controlled two immune-evading VoCs, the Beta (B.1.135) and the Omicron (BA.1) variants in BALB/c mice, and S-specific immunity was maintained for at least 5 months after immunization, where neutralizing titers against all tested VoCs were higher at 5-months than at 1-month post-vaccination. Thus, cytomegalovirus (CMV)-based vector vaccines might allow for long-term protection against COVID-19.**

## Introduction

The severe acute respiratory coronavirus-2 (SARS-CoV-2) emerged in Hubei province, China, in 2019 [1]. Since then, the virus has spread worldwide and caused the ongoing COVID-19 pandemic. Although SARS-CoV-2 was genetically largely stable during the initial months of the pandemic, several variants of concern (VoCs) have emerged in the meantime and present an increased threat to global public health [2] due to their augmented transmissibility and/or antibody escape [3,4].

In the European Union, six vaccines are currently approved for administration in humans [5], including two mRNA-based vaccines, two vector-based vaccines, one adjuvanted protein vaccine, and an inactivated

virus vaccine. All authorized vaccines induce humoral immune responses against the spike (S) glycoprotein of SARS-CoV-2, which drives viral entry into cells and is the key target for neutralizing antibodies. However, vaccine-induced immunity wanes within months, resulting in reduced protection against infections and disease[6-8]. Consequently, booster shots were recommended, but they also do not confer long-term protection against infection and disease, especially in light of novel immune-evasive VoCs, such as the Beta variant [8], or the currently dominating Omicron VoC (Pango lineage B.1.1.529) [9]. Therefore, the need for a vaccine that confers long-lasting and broad immune protection remains unmet.

Murine cytomegalovirus (MCMV) belongs to the *betaherpesvirinae* subfamily and is a well-studied model virus for human CMV (HCMV) infection [10]. CMVs induce uniquely robust anti-viral immunity, which persists over a lifetime [11,12]. This long-term maintenance of antigen-specific lymphocytes, known as memory inflation [13,14], is characterized by an accumulation and persistence of CD8 T cells with an effector memory ($T_{EM}$) phenotype, recognizing immunodominant viral antigens [13,15]. Therefore, CMV has been explored as a vaccine vector that provides long-term immune protection against many infectious targets, based on a peculiarly strong CD8 T cell immunity [16-21]. MCMV infection also results in lasting humoral immune responses toward viral antigens [22], which can be exploited to retarget immune protection against other viruses [23]. Mouse models of SARS-CoV-2 infection for preclinical vaccine efficacy testing were initially restricted to transgenic mice expressing the human ACE2 receptor (hACE2), or mouse-adapted SARS-CoV-2 variants because the original strains of SARS-CoV-2 could not bind to mouse ACE2 (mACE2) receptors. However, the N501Y mutation in the S protein observed in various VoCs, including Beta and Omicron VoCs, allows mACE2 binding [24] and wild type (WT) mice infection, enabling the analysis of SARS-CoV-2 infection in the absence of exogenous receptor expression [25].

Recently, our group has demonstrated that an MCMV-based COVID-19 vaccine candidate encoding the S protein from the Wuhan prototype ($MCMV^S$) induced long-lasting humoral and cellular immunity [26]. Here, we show that immunization with $MCMV^S$ protects vaccinated K18-hACE2 mice against a lethal dose of the SARS-CoV-2 D614G strain. Furthermore, the same vaccination protects BALB/c mice against viral challenge with the immune-evasive Beta and Omicron strains, and the protection persists for at least 5 months with no signs of immune waning because immunity, particularly virus neutralizing titer (VNT), at 5 months was even stronger than at 5 weeks post-vaccination. Hence, our results argue that CMV-based SARS-CoV-2 vaccines may provide long-term and broad protection against multiple VOCs.

## Results

### Immune responses of $MCMV^S$–vaccinated K18-hACE2 mice

We have previously shown that $MCMV^S$ immunization of BALB/c and C57BL/6 mice elicits a strong humoral response as well as an inflationary CD8 T cell response towards the S antigen, respectively [26]. Here, we immunized K18-hACE2 mice intraperitoneally (i.p.) with either $MCMV^S$, $MCMV^{WT}$, or PBS and challenged them one or three months later with a lethal dose of a SARS-CoV-2 D614G strain (**Fig. 1A**). Mice were bled 7 days before the SARS-CoV-2 challenge, and blood leukocytes were analyzed by flow cytometry (gating strategy shown in **Supplementary Fig. 1**). $MCMV^S$ and $MCMV^{WT}$ elicited comparable levels of CD8 T cells in total, primed, effector ($T_{EFF}$), terminally differentiated effector ($T_{TDE}$), effector memory ($T_{EM}$), and central memory ($T_{CM}$) compartments in short-term (1 month) and long-term (3 months) groups (**Fig. 1B** and **supplementary Fig. 2**). We noticed that a single mouse in the short-term group exhibited a very low frequency of primed CD8 T cells, possibly an indication of a technical failure. This animal is shown for transparency and was marked with an X symbol (**Fig. 1B**, X -marked symbols).

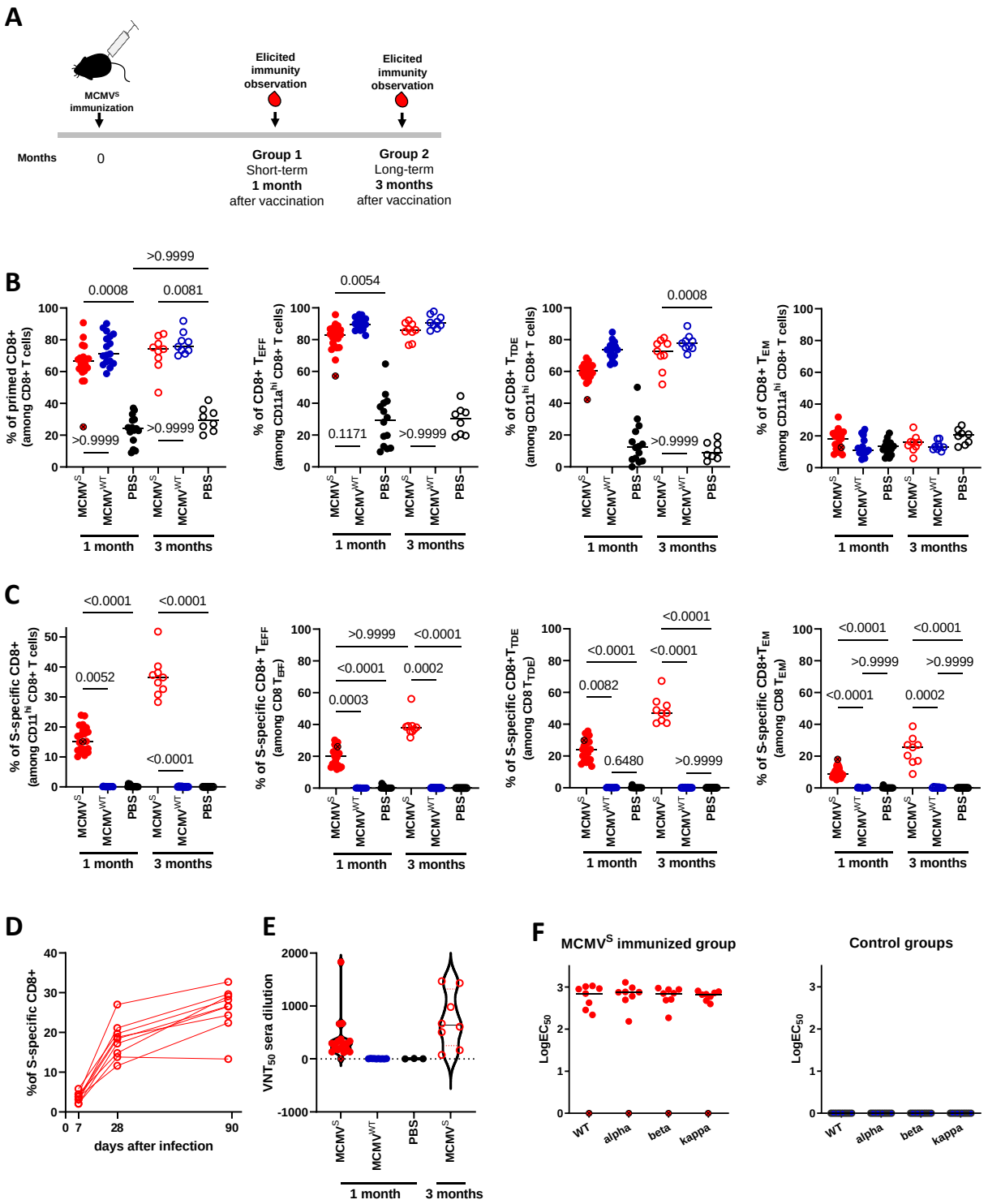


***Figure 1. Immune status of MCMV$^S$–vaccinated K18-hACE2 mice***

*(A) Schematic image of the experimental setup. (B) CD3+CD8+CD4- T cells were gated for the primed subpopulation (CD11$^{hi}$CD44$^{hi}$ – leftmost panel). Primed CD8 T cells were progressively gated into $T_{EFF}$ (CD62L$^{lo}$), $T_{TDE}$ (CD62L$^{lo}$KLRG1$^{hi}$), or $T_{EM}$ (CD62L$^{lo}$KLRG1$^{lo}$) subpopulations. Frequencies of cells in each subset as a fraction of the parental population are shown. Horizontal lines show the median. (C) The percentages of S-specific cells in each subset shown in B are shown. (B,C) Each symbol is an individual animal; the MCMV$^S$-vaccinated animal with poor immune responses is marked with an X. Horizontal lines denote medians. Kruskal-Wallis tests were used for the statistical analyses (n=21 MCMV$^S$, n=15 MCMV$^{WT}$, PBS for 1-month; n=9 MCMV$^S$, MCMV$^{WT}$, n=8 PBS for 3-*

*months). (D) Antigen-specific memory responses over time in blood shown as the percentage of antigen-specific cells within the total CD8 compartment. Each line connects values from an individual mouse at indicated time points. (E) Violin plots of VNTs that resulted in a 50% of reduction of SARS-CoV-2 infection ($VNT_{50}$). Each symbol indicates an individual mouse. (F) $EC_{50}$ of the IgG fraction specific for the respective S antigens from indicated variants measured by ELISA. Each symbol indicates an individual mouse and each color represents vaccination with following vectors: Red=$MCMV^S$, Blue=$MCMV^{WT}$, and Black=PBS. Horizontal lines show geometric means. One $MCMV^S$-vaccinated animal with poor immune responses is marked with an X throughout.*

Importantly, only $MCMV^S$-vaccinated K18-hACE2 mice displayed high frequencies of CD8 cells recognizing the antigenic epitope VNFNFNGL of the S protein, while control groups showed no S-specific T-cell immunity (**Fig. 1B** and **C**). The long-term cohort showed a ~ two-fold increase of S-specific T-cells in all examined subsets over the short-term cohort (**Fig. 1C**), and dynamic monitoring of S-specific CD8 T cells in the peripheral blood confirmed a strong inflationary response at single animal level (**Fig. 1D**), in line with our previous report in C57BL/6 mice [26]. We also observed an increase in average neutralizing antibody titers in the sera of long-term $MCMV^S$-vaccinated animals (**Fig. 1E**). Vaccinated mice showed high titers of anti-S IgGs, which recognized various variants of interest and concern. Sera of mice mock-immunized with $MCMV^{WT}$ or PBS did not show any S-specific antibody response (**Fig. 1E** and **F**), arguing strongly that the responses were not due to cross-reactions against potential MCMV antigens. Overall, these results indicated that $MCMV^S$ vaccination induces potent and lasting adaptive immunity towards the S antigen.

## Protection against SARS-CoV-2 challenge after a single vaccine dose

A week after the analysis shown in **Fig. 1**, short-term vaccinated K18-hACE2 mice were challenged with $2x10^3$ PFU of SARS-CoV-2 (B.1 strain, D614G mutation), and daily monitored for weight loss and disease indicators (**Fig. 2A**). All $MCMV^S$-immunized animals that robustly responded to vaccination (**Fig. 1B** and **1F**) were protected from clinical signs and weight loss, while mock-vaccinated mice became severely ill, reaching the humane end-point by day 5 post-infection or earlier (**Fig. 2B** and **2C**). $MCMV^S$-immunized mice survived the lethal SARS-CoV-2 challenge, even when monitored for 3 weeks (**Fig. 2D** and **Supplementary Fig. 3**).

SARS-CoV-2 can infect a broad range of tissues in K18-hACE2 mice as well as in humans [27,28]. Therefore, we tested whether $MCMV^S$ vaccination decreases the SARS-CoV-2 viral load in the trachea, lungs, stomach, brain, heart, and spleen (**Fig. 2E**). In all organs, $MCMV^S$-vaccinated animals showed reduced SARS-CoV-2 viral RNA load for up to 3 weeks, while mock-vaccinated groups exhibited high viral RNA copy numbers (**Fig. 2F** and **Supplementary Fig.4**). In particular, $MCMV^S$ vaccination reduced viral load in the trachea and lungs by roughly a 1,000-fold (**Fig. 2F**, trachea and lungs) and also markedly reduced viral loads in the CNS (**Fig. 2F**, brain), which is known to be targeted by the virus in K18-hACE2 mice [27,28]. The viral burden in other organs showed a similar pattern with a strong decrease of detectable SARS-CoV-2 RNAs in $MCMV^S$-immunized animals at 7 days post-infection (dpi) in comparison with the control groups, where viral RNA persisted until 7 dpi (**Fig. 2F**, stomach, heart, and spleen). To sum up, $MCMV^S$ immunization protected animals from developing clinical signs and high viral loads in all organs tested.

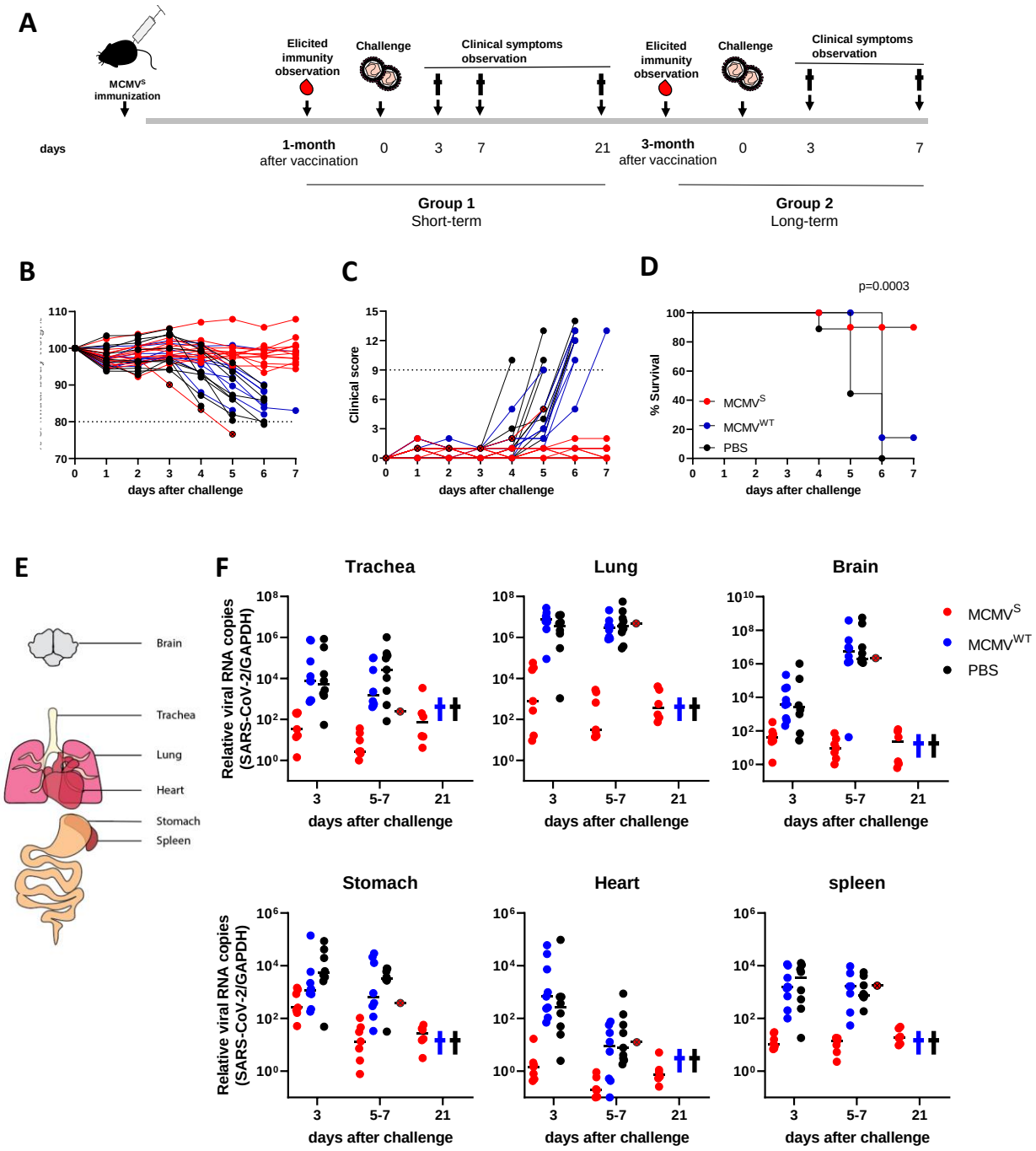


***Figure 2. Short-term protection elicited by MCMV$^S$ vaccination***

*(A) Schematic image of experimental setup. (B) Percentage of body weight and (C) daily clinical scores upon challenge are shown. The dotted line indicates the threshold in score resulting in a humane end-point. (D) Mock-survival kinetics of challenged mice representing the % of mice reaching a humane end point. A log-rank (Mantel-cox) test* was used for the statistical analysis. *(E) Schematic illustration of the organs that were collected for virological analyses. (F) Relative viral RNA loads in the representative organs at the indicated time points normalized to the housekeeping gene mGAPDH. Cross symbols indicate no animals alive by the time of analyses. Horizontal lines indicate medians. The outlier animal with poor immunity is marked with an X-marked red dot throughout. Organs of mock-immunized mice that reached humane end-points before 7 days upon challenge were harvested on the day of euthanasia. Pooled data (n=6-8 per group) from two independent experiments are shown (except for the 21 days data set, which was generated once).*

## Protection against SARS-CoV-2 challenge three months after vaccination

The sera/plasma of convalescent COVID-19 patients contains anti-S antibodies, which begin to diminish around 28 days after infection [29,30]. Similarly, clinically approved vaccines elicit immunity that wanes over time, and hence, durable immunity elicited by vaccines against COVID-19 is an unmet need. To define the long-term immune protection upon MCMV$^{S}$ vaccination, K18-hACE2 mice were challenged with SARS-CoV-2 D614G strain three months after vaccination and daily monitored for clinical scores (**Fig. 2A**). All MCMV$^{S}$-vaccinated mice were protected against SARS-CoV-2 infection, uniformly surviving, maintaining their weights and showing no noticeable symptoms (**Fig. 3A**). Viral RNA burdens were reduced in the MCMV$^{S}$-immunized group in all examined organs. A few mice showed remaining viral RNA detected in the respiratory and gastrointestinal tracts, but only minor amounts of viral RNAs were detected in other organs (**Fig. 3B** and **Supplementary Fig. 5**), arguing that a single administration of the MCMV$^{S}$ vaccine protects mice for at least 3 months.

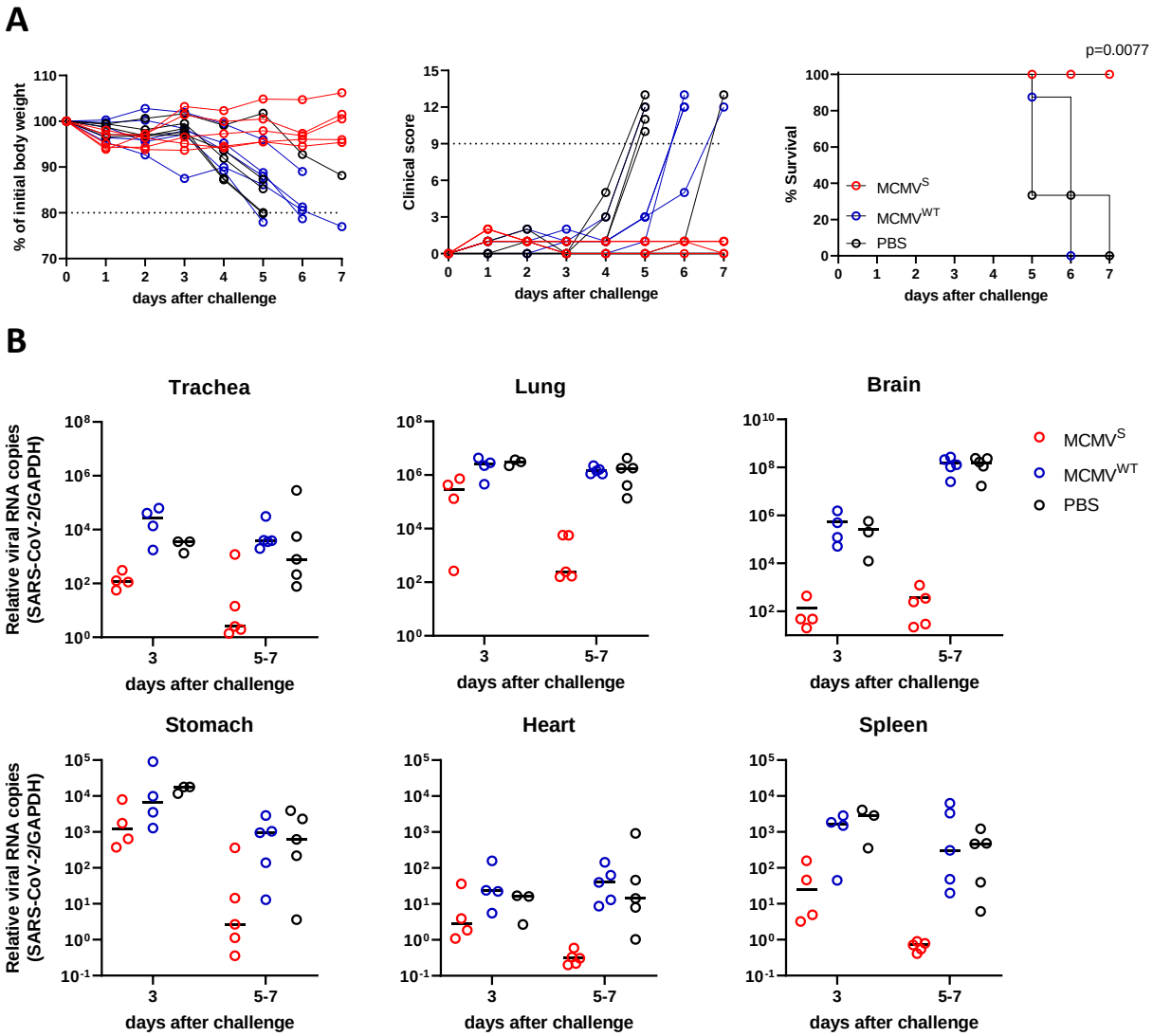


***Figure 3. Long-term protection elicited by MCMV$^{S}$ vaccination against SARS-CoV-2***

*(A) Percentage of body weight (left), daily clinical scores (middle), and mock-survival kinetics of challenged mice representing the % of mice reaching a humane end point (right). Log-rank (Mantel-cox) test* was used for the statistical analysis (n=5 each). *(B)*

*Relative viral RNA loads in the representative organs at the indicated time points, normalized to GAPDH. In mice that reached humane endpoints, organs were harvested on the day of euthanasia. Each symbol is an individual mouse, and horizontal lines indicate the median of biological replicates.*

## Sustained neutralizing antibody responses against Beta and the Omicron variants upon $MCMV^S$ immunization

While our data on protection were encouraging, the emergence of immune-evading SARS-CoV-2 VoCs compelled an examination of the protective ability of our MCMV-based vaccine against representative VoCs. To this end, we conducted vaccine efficacy studies against the Beta (B.1.351) and the Omicron variant (BA.1). Unlike the D614G strain, both VoCs contain the N501Y mutation in the S protein, which allows SARS-CoV-2 infection in common inbred mice, such as BALB/c and C57BL/6 [24]. The prototype S protein, present in $MCMV^S$, binds to hACE2 but does not bind to mACE2 [31]. Hence, by immunizing BALB/c mice, we evaluated the efficacy of a vaccine formulation that does not engage the mACE2 receptor and has potentially fewer side effects. Moreover, to assess whether our vaccine can protect animals for more than 3 months, we challenged the long-term cohort at 5-months post-vaccination. A short-term cohort was challenged at 6 weeks after immunization as a point of reference. One week before the SARS-CoV-2 challenge, all mice were bled for immune status analyses.

Virus-neutralizing titers were examined by the pseudo-neutralization assay using pseudotyped VSV (pVSV) that expressed S antigens from the Wuhan, the Beta, or the Omicron variant at 1 or 5 months post-immunization. The neutralization capacity of sera was expressed as the titer resulting in 50% of pseudovirus neutralization ($pVNT_{50}$), and a head-to-head comparison of $pVNT_{50}$ against Wuhan and Beta (**Fig. 4A**) or Wuhan and Omicron VoCs (**Fig. 4B**) was performed at 5 months post-vaccination. While $pVNT_{50}$ values against both variants were reduced in most samples, the reduction of titers was less pronounced in Beta (**Fig. 4A**) than in the Omicron variant (**Fig. 4B**), consistent with previous clinical observations [32]. The neutralizing capacity was not due to cross-neutralizing effects against the vector, because sera from animals immunized with the $MCMV^{WT}$ did not neutralize the pseudoviruses (**Fig. 4A** and **4B**). Strikingly, monitoring for immune waning by comparison of the neutralizing capacity at 5 weeks and 5 months post-immunization revealed that $pVNT_{50}$ did not decrease but rather increased from 5 weeks to 5 months post-immunization, and this was observed for all tested VoCs (**Fig. 4C**). Taken together, an MCMV-based vaccine expressing a receptor-non-binding S antigen elicited strong and long-lasting neutralizing antibody responses.

## Reduced viral loads in animals at 1 and 5 months after $MCMV^S$ immunization and challenge with Beta and Omicron variants

A week after the bleeding, animals were challenged with $6x10^4$ PFU of the Beta or the Omicron variant of SARS-CoV-2, and vaccine efficacy as determined by the reduction of viral burdens was measured. For this, we analyzed viral RNA copies and infectivity in the lung at 3 days post-infection. We chose this setup since infectious SARS-CoV-2 particles are only detectable for 3 days in the lungs and largely absent from extrapulmonary organs [27,33,34]. $MCMV^S$-immunized animals harbored fewer infectious particles in the lungs as compared to the $MCMV^{WT}$ control group (**Fig. 4D**). Parallel viral load analyses indicated that the short-term cohort (1 month) had on average higher residual viral RNAs than the long-term cohort (5 months) (**Fig. 4E**). However, three animals in the 5-months post-vaccination group showed high viral RNA loads upon infection with the Beta VoC and two of the samples were also highly infectious (**Fig. 4D**). These animals exhibited weak or undetectable neutralization against any tested variant (**Fig. 4C**), implying poor vaccination response or vaccination failure in a subset of animals. $MCMV^S$-vaccinated animals also

controlled replication of the Omicron variant based on viral load, which was 100-fold reduced in the short-term cohort and 10,000-fold in the long-term challenge scenario (**Fig. 4G**). Isolation of infectious Omicron virus was not successful for unclear reasons at present. Taken together, our results are consistent with long-lasting and improving adaptive immunity against the S antigen over time upon vaccination with MCMV$^S$ (**Fig. 1C, 1E,** and **4C**).

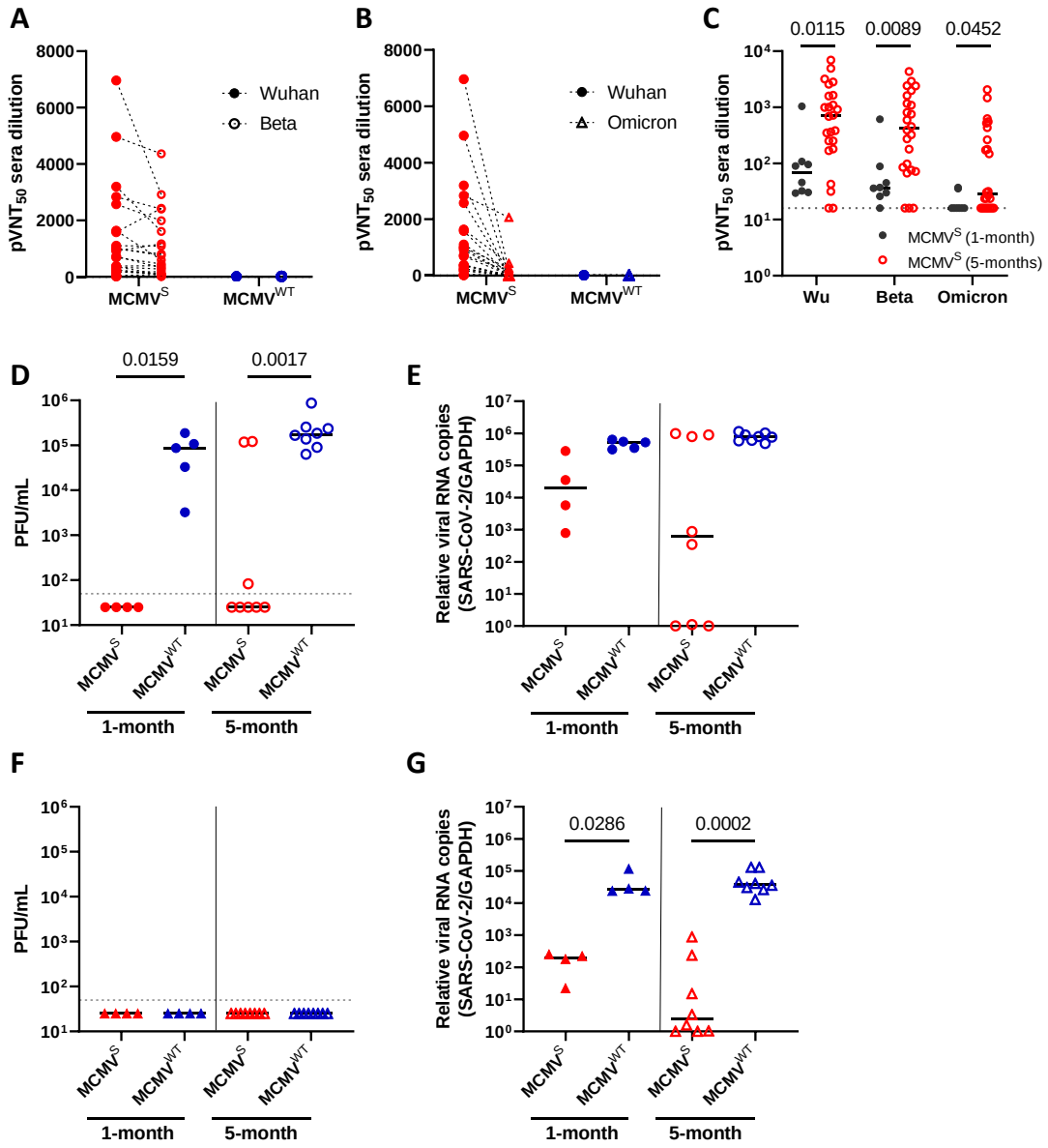


***Figure 4. Beta- and Omicron-specific neutralizing antibodies and in vivo control at 1 and 5 months post-MCMV$^S$ immunization*** *(A-B) pVNT$_{50}$ from the same mice at 5 months post-vaccination (A) against the Wuhan and Beta VoC or (B) Wuhan and Omicron VoC are connected by dashed lines (n=24). (C) Dot plots of pVNT$_{50}$ against each variant from the sera of the 1-month (n=8) and 5-months cohorts (n=24). Each symbol indicates an individual mouse. Solid horizontal lines show the median and the dotted line indicates the detection limit. (D) Infectious virus titers in lungs of SARS-CoV-2 Beta-challenged mice. (E) Relative viral RNA loads in lungs of SARS-CoV-2 Beta-challenged mice normalized to GAPDH. (F) Infectious virus titers in lungs of SARS-CoV-2 Omicron-challenged mice. (G) GAPDH normalized viral RNA loads in lungs of Omicron-challenged mice. Each symbol indicates an individual mouse, and solid horizontal lines indicate the median of biological replicates. Dashed lines indicate limits of detection. Two-tailed Mann-Whitney tests were used for statistical analysis (n=4 MCMV$^S$, n=5 MCMV$^{WT}$ for 1-month; n=8 each for 5-months).*

## Protection against SARS-CoV-2-associated illness against immune-evasive Beta VoC

Next, we assessed protection against disease development upon challenge with the Beta or Omicron VoC. In groups challenged 1-month post-vaccination with the Beta variant, MCMV$^{S}$-immunized animals retained their weights and displayed few clinical symptoms, while MCMV$^{WT}$ mock-immunized animals lost around 10% of their initial weights (**Fig. 5A-C**). Similarly, MCMV$^{S}$-vaccinated animals were overall protected from weight loss in comparison with MCMV$^{WT}$-controls at 5-months post-vaccination (**Fig. 5D**) and displayed lower clinical scores (**Fig. 5E** and **5F**). A randomly pre-selected subset of animals was monitored for 7 days, where 50% of animals in the mock-immunized group reached the humane end-point, while body weights were maintained in all MCMV$^{S}$-vaccinated animals (**Fig. 5G**). Animals that were challenged with the Omicron variant showed no weight loss and very mild clinical symptoms (**Supplementary Fig. 6**), in line with reports by other studies. Animals vaccinated with MCMV$^{S}$ for 5 months were nevertheless protected against the mild symptoms elicited by the Omicron infection, because the cumulative clinical scores at dpi 3 were on average 2-fold lower in this than in the MCMV$^{WT}$ control group. Altogether, our data strongly indicate that a single dose of MCMV$^{S}$ vaccination provides long-lasting protection against the immune evasive Beta variant of SARS-CoV-2.

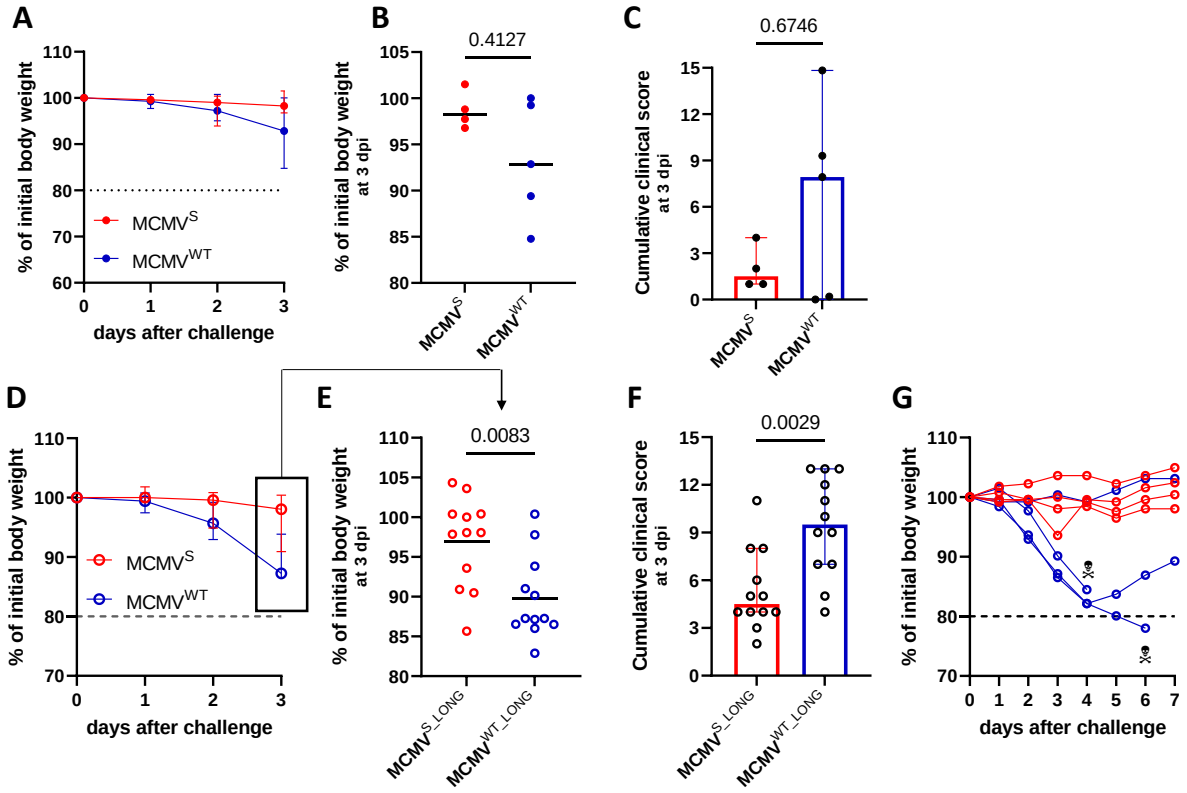


***Figure 5. Protection against the Beta variant-associated illness after 1-month or 5-months after vaccination***

*(A, D) Percentage of body weight monitored for 3 days after upon infection with the Beta variant. Medians with 95% confidence interval are shown. (B, E) Percentages of initial body weight in individual animals at 3 dpi. Each symbol indicates an individual mouse. (C, F) Cumulative clinical scores at dpi 3. Each symbol shows summed-up clinical scores up to 3 dpi. Medians (bar graphs) with 95% confidence interval are shown. (G) Body weight loss was monitored for a week after the SARS-CoV-2 infection. Each line connecting dots indicates an individual mouse, and skull symbols indicate animals that reached a humane end-point. Closed symbols show one month (A-C) and open symbols present five months (D-G) after vaccination. Dashed lines indicate the humane-end point. Solid horizontal lines show the median of biological replicates (n=4 MCMV$^{S}$, n=5 MCMV$^{WT}$ for A-C; n=12 each for D-F). Statistical significance was analyzed using two-tailed Mann-Whitney tests.*

## Discussion

Several vaccines have been developed to combat the COVID-19 pandemic. However, immune waning remains an unresolved problem [6,7,9,35], and vaccines that result in lasting and broad protection against SARS-CoV-2 variants remain unavailable. The emergence of the Omicron variant has emphasized the urgent need for such a vaccine, as the currently authorized vaccine regimens showed heterogeneous protection levels against this variant [36,37], resulting in 30-88% of vaccine effectiveness against hospitalization and frequent breakthrough infections [38]. Viral vectors that were authorized early in the COVID-19 pandemic, such as Vaxzevria (ChAdOx1-S) and the COVID-19 vaccine Janssen (Ad26.COV2.S) [39], exhibit the same restrictions as the mRNA-based vaccines [36]. CMV has received attention as a new vaccine vector tool due to the induction of a strong and lasting T-cell immunity [21]. While HCMV seroprevalence is estimated to exceed 90% in some geographic areas, the pre-existing immunity to CMV does not hinder vaccine responses and protection, as demonstrated in studies with rhesus monkeys [17,40]. MCMV shares structural and functional homology with HCMV and allows *in vivo* analyses in the natural host. Hence, we used this model virus to test whether a CMV-based vector might in principle induce long-lasting protection against SARS-CoV-2 infection and disease development. Our vaccine induced strong and durable S-specific CD8 T cells (**Fig. 1C-D**) and neutralizing antibody responses (**Fig. 1E** and **4C**). Importantly, immune protection against lethal challenge at 3 months post-immunization (**Fig. 3**) was just as robust as at 1-month post-infection (**Fig. 2**) and protection against immune evasive VoCs was maintained at 5 months post-vaccination (**Fig. 4** and **5**). Hence, our data indicate that our approach may provide durable immune protection against COVID-19 upon vaccination.

Neutralizing antibody responses correlate with vaccine effectiveness [41] and are therefore considered an important predictor of vaccine potency. We have previously shown that MCMV-based vaccines may elicit strong antibody responses whose affinity and neutralizing capacity increase over time [26]. Here, we show that the MCMV$^{S}$ vaccine induces antibodies that neutralize the Beta and Omicron variants and protect against disease upon infection with these viruses, with neutralization titers increasing over time (**Fig. 4A-C**). This feature is unique for our vaccine approach and in stark contrast with other vaccine formulations, which require prime/boost administration for optimal performance [39,42,43]. Considering that neutralizing antibodies against SARS-CoV-2 wane at similar rates upon infection or vaccination with currently used vaccines [30,35,37,44], our vaccine provides an improvement over both of these scenarios.

Interestingly, even the vaccinated animals with weak neutralizing antibody responses against SARS-CoV-2 variants were protected against illness and showed lowered viral loads in the lungs (**Fig. 4**). This phenomenon was also demonstrated in a preclinical study with rhesus macaques and in clinical studies, where study subjects were protected although no neutralizing antibodies were observed [45-47]. One may speculate that T-cell immunity elicited by MCMV$^{S}$ vaccination protected these animals, but we cannot exclude the possibility that memory B lymphocytes in MCMV$^{S}$-immunized mice responded to the challenge by rapidly generating neutralizing antibodies upon challenge, thus limiting virus replication and protecting the host. It is finally also possible that the concerted action of these two lymphocyte lineages protected the vaccinated mice against challenge. To differentiate between these scenarios, one may use MCMV vectors eliciting T-cell responses against S epitopes only, or mice lacking T-cells, but these experiments go beyond the scope of our study.

In this study, we showed that an S antigen that cannot bind to the target ACE2 receptor might still provide robust immune protection. Namely, we cloned the S antigen from the prototypical Wuhan strain of SARS-

277 CoV-2 into our vaccine vector, but the binding affinity of the Wuhan S protein to murine ACE2 receptors
278 is low [31]. Consequently, the S antigen from our vaccine could not bind to the mACE2 receptor. On the
279 other hand, the N501Y mutation in the S protein enables infection of common laboratory inbred mice,
280 such as BALB/c or C57BL/6 [24], and this mutation is present in the Beta and the Omicron VoCs. Therefore,
281 $MCMV^S$ elicited protective immunity against variants that engaged the mACE2, although the S expressed
282 by the vaccine vector did not. This is interesting because some studies reported that the binding of the S1
283 subunit of the S protein to ACE2 on endothelial cells may affect endothelial barrier integrity and cardiac
284 activity [48-50]. While we cannot formally exclude that long-term S antigen expression may drive adverse
285 effects unrelated to ACE2 biding, our data demonstrate that our vaccine formulation protects mice against
286 SARS-CoV-2 variants in absence of ACE2 receptor engagement, which is especially important if low levels
287 of S antigen persist in the host.

288 The data presented here demonstrate that an MCMV-based vaccine candidate expressing the full-length
289 prototype S protein is highly immunogenic and protective in mice, with robust activation of both arms of
290 the adaptive immune system, cellular and humoral responses. We demonstrated robust protection
291 against a lethal dose of the SARS-CoV-2 D614G variant in K18-hACE2 mice and the immune-evasive Beta
292 and Omicron variants in BALB/c mice by a single dose of our $MCMV^S$ vaccine. Future research needs to
293 focus on a head to head comparison of CMV-based vaccines with other COVID-19 vaccine formulations,
294 on the length of protection and administration routes, paving the way towards clinical trials with
295 appropriate CMV vectors. However, by demonstrating in proof of concept that a CMV vector can provide
296 long-term protection against COVID-19 upon a single immunization shot, we provide here the first and
297 crucial step in this direction.

## 298 Reference


299 1 Andersen, K. G., Rambaut, A., Lipkin, W. I., Holmes, E. C. & Garry, R. F. The proximal origin of SARS-
300 CoV-2. *Nat Med* **26**, 450-452, doi:10.1038/s41591-020-0820-9 (2020).
301 2 WHO. in *World Health Organization* (2022).
302 3 Korber, B. *et al.* Tracking Changes in SARS-CoV-2 Spike: Evidence that D614G Increases Infectivity
303 of the COVID-19 Virus. *Cell* **182**, 812-827 e819, doi:10.1016/j.cell.2020.06.043 (2020).
304 4 Hoffmann, M. *et al.* SARS-CoV-2 variants B.1.351 and P.1 escape from neutralizing antibodies. *Cell*
305 **184**, 2384-2393 e2312, doi:10.1016/j.cell.2021.03.036 (2021).
306 5 PEI. in *PEI* (2022).
307 6 Shrotri, M. *et al.* Spike-antibody waning after second dose of BNT162b2 or ChAdOx1. *Lancet* **398**,
308 385-387, doi:10.1016/S0140-6736(21)01642-1 (2021).
309 7 Levin, E. G. *et al.* Waning Immune Humoral Response to BNT162b2 Covid-19 Vaccine over 6
310 Months. doi:10.1056/NEJMoa2114583 (2021).
311 8 Pegu, A. *et al.* Durability of mRNA-1273 vaccine-induced antibodies against SARS-CoV-2 variants.
312 **373**, 1372-1377, doi:doi:10.1126/science.abj4176 (2021).
313 9 Schubert, M. *et al.* Human serum from SARS-CoV-2-vaccinated and COVID-19 patients shows
314 reduced binding to the RBD of SARS-CoV-2 Omicron variant. *BMC Med* **20**, 102,
315 doi:10.1186/s12916-022-02312-5 (2022).
316 10 Fisher, M. A. & Lloyd, M. L. A Review of Murine Cytomegalovirus as a Model for Human
317 Cytomegalovirus Disease-Do Mice Lie? *Int J Mol Sci* **22**, doi:10.3390/ijms22010214 (2020).
318 11 Sylwester, A. W. *et al.* Broadly targeted human cytomegalovirus-specific CD4+ and CD8+ T cells
319 dominate the memory compartments of exposed subjects. *J Exp Med* **202**, 673-685,
320 doi:10.1084/jem.20050882 (2005).

321 12 Klenerman, P. & Oxenius, A. T cell responses to cytomegalovirus. *Nature reviews. Immunology* **16**,
322 367-377, doi:10.1038/nri.2016.38 (2016).
323 13 Holtappels, R., Pahl-Seibert, M. F., Thomas, D. & Reddehase, M. J. Enrichment of immediate-early
324 1 (m123/pp89) peptide-specific CD8 T cells in a pulmonary CD62L(lo) memory-effector cell pool
325 during latent murine cytomegalovirus infection of the lungs. *J Virol* **74**, 11495-11503 (2000).
326 14 Karrer, U. *et al.* Memory inflation: continuous accumulation of antiviral CD8+ T cells over time.
327 *Journal of immunology* **170**, 2022-2029 (2003).
328 15 Cicin-Sain, L. Cytomegalovirus memory inflation and immune protection. *Medical microbiology*
329 *and immunology* **208**, 339-347, doi:10.1007/s00430-019-00607-8 (2019).
330 16 Morabito, K. M. *et al.* Intranasal administration of RSV antigen-expressing MCMV elicits robust
331 tissue-resident effector and effector memory CD8+ T cells in the lung. *Mucosal immunology* **10**,
332 545-554, doi:10.1038/mi.2016.48 (2017).
333 17 Hansen, S. G. *et al.* A live-attenuated RhCMV/SIV vaccine shows long-term efficacy against
334 heterologous SIV challenge. *Sci Transl Med* **11**, doi:10.1126/scitranslmed.aaw2607 (2019).
335 18 Zheng, X. *et al.* Mucosal CD8+ T cell responses induced by an MCMV based vaccine vector confer
336 protection against influenza challenge. *PLoS Pathog* **15**, e1008036,
337 doi:10.1371/journal.ppat.1008036 (2019).
338 19 Slavuljica, I. *et al.* Recombinant mouse cytomegalovirus expressing a ligand for the NKG2D
339 receptor is attenuated and has improved vaccine properties. *J Clin Invest* **120**, 4532-4545,
340 doi:10.1172/JCI43961 (2010).
341 20 Tsuda, Y. *et al.* A replicating cytomegalovirus-based vaccine encoding a single Ebola virus
342 nucleoprotein CTL epitope confers protection against Ebola virus. *PLoS Negl Trop Dis* **5**, e1275,
343 doi:10.1371/journal.pntd.0001275 (2011).
344 21 Karrer, U. *et al.* Expansion of protective CD8+ T-cell responses driven by recombinant
345 cytomegaloviruses. *J Virol* **78**, 2255-2264, doi:10.1128/jvi.78.5.2255-2264.2004 (2004).
346 22 Welten, S. P. M., Redeker, A., Toes, R. E. M. & Arens, R. Viral Persistence Induces Antibody Inflation
347 without Altering Antibody Avidity. *J Virol* **90**, 4402-4411, doi:10.1128/jvi.03177-15 (2016).
348 23 Bongard, N. *et al.* Immunization with a murine cytomegalovirus based vector encoding retrovirus
349 envelope confers strong protection from Friend retrovirus challenge infection. *PLoS Pathog* **15**,
350 e1008043, doi:10.1371/journal.ppat.1008043 (2019).
351 24 Gu, H. *et al.* Adaptation of SARS-CoV-2 in BALB/c mice for testing vaccine efficacy. *Science (New*
352 *York, N.Y.)* **369**, 1603-1607, doi:10.1126/science.abc4730 (2020).
353 25 Tian, F. *et al.* N501Y mutation of spike protein in SARS-CoV-2 strengthens its binding to receptor
354 ACE2. *eLife* **10**, e69091, doi:10.7554/eLife.69091 (2021).
355 26 Kim, Y. *et al.* MCMV-based vaccine vectors expressing full-length viral proteins provide long-term
356 humoral immune protection upon a single-shot vaccination. *Cell Mol Immunol* **19**, 234-244,
357 doi:10.1038/s41423-021-00814-5 (2022).
358 27 Yinda, C. K. *et al.* K18-hACE2 mice develop respiratory disease resembling severe COVID-19.
359 *bioRxiv*, doi:10.1101/2020.08.11.246314 (2020).
360 28 Oladunni, F. S. *et al.* Lethality of SARS-CoV-2 infection in K18 human angiotensin-converting
361 enzyme 2 transgenic mice. *Nat Commun* **11**, 6122, doi:10.1038/s41467-020-19891-7 (2020).
362 29 Seow, J. *et al.* Longitudinal observation and decline of neutralizing antibody responses in the three
363 months following SARS-CoV-2 infection in humans. *Nature Microbiology* **5**, 1598-1607,
364 doi:10.1038/s41564-020-00813-8 (2020).
365 30 Marcotte, H. *et al.* Immunity to SARS-CoV-2 up to 15 months after infection. *iScience* **25**, 103743,
366 doi:10.1016/j.isci.2022.103743 (2022).
367 31 Zhou, P. *et al.* A pneumonia outbreak associated with a new coronavirus of probable bat origin.
368 *Nature* **579**, 270-273, doi:10.1038/s41586-020-2012-7 (2020).

32 Bekliz, M. *et al.* Neutralization capacity of antibodies elicited through homologous or heterologous infection or vaccination against SARS-CoV-2 VOCs. *Nature Communications* **13**, 3840, doi:10.1038/s41467-022-31556-1 (2022).
33 Muruato, A. *et al.* Mouse-adapted SARS-CoV-2 protects animals from lethal SARS-CoV challenge. *PLoS Biol* **19**, e3001284, doi:10.1371/journal.pbio.3001284 (2021).
34 Sun, S. *et al.* Characterization and structural basis of a lethal mouse-adapted SARS-CoV-2. *Nature Communications* **12**, 5654, doi:10.1038/s41467-021-25903-x (2021).
35 Widge, A. T. *et al.* Durability of Responses after SARS-CoV-2 mRNA-1273 Vaccination. **384**, 80-82, doi:10.1056/NEJMc2032195 (2020).
36 Andrews, N. *et al.* Covid-19 Vaccine Effectiveness against the Omicron (B.1.1.529) Variant. **386**, 1532-1546, doi:10.1056/NEJMoa2119451 (2022).
37 Ferdinands, J. M. *et al.* Waning 2-Dose and 3-Dose Effectiveness of mRNA Vaccines Against COVID-19-Associated Emergency Department and Urgent Care Encounters and Hospitalizations Among Adults During Periods of Delta and Omicron Variant Predominance - VISION Network, 10 States, August 2021-January 2022. *MMWR Morb Mortal Wkly Rep* **71**, 255-263, doi:10.15585/mmwr.mm7107e2 (2022).
38 International Vaccine Access Center (IVAC), J. H. B. S. o. P. H. Resource Library. *VIEW-hub* (2022). <www.view-hub.org.>.
39 Tregoning, J. S. *et al.* Vaccines for COVID-19. *Clin Exp Immunol* **202**, 162-192, doi:10.1111/cei.13517 (2020).
40 Hansen, S. G. *et al.* Effector memory T cell responses are associated with protection of rhesus monkeys from mucosal simian immunodeficiency virus challenge. *Nat Med* **15**, 293-299, doi:10.1038/nm.1935 (2009).
41 Khoury, D. S. *et al.* Neutralizing antibody levels are highly predictive of immune protection from symptomatic SARS-CoV-2 infection. *Nat Med* **27**, 1205-1211, doi:10.1038/s41591-021-01377-8 (2021).
42 Carazo, S. *et al.* Single-Dose Messenger RNA Vaccine Effectiveness Against Severe Acute Respiratory Syndrome Coronavirus 2 in Healthcare Workers Extending 16 Weeks Postvaccination: A Test-Negative Design From Québec, Canada. *Clinical Infectious Diseases*, doi:10.1093/cid/ciab739 (2021).
43 Tscherne, A. *et al.* Immunogenicity and efficacy of the COVID-19 candidate vector vaccine MVA-SARS-2-S in preclinical vaccination. **118**, e2026207118, doi:doi:10.1073/pnas.2026207118 (2021).
44 Lau, E. H. *et al.* Long-term persistence of SARS-CoV-2 neutralizing antibody responses after infection and estimates of the duration of protection. *EClinicalMedicine* **41**, 101174, doi:10.1016/j.eclinm.2021.101174 (2021).
45 McMahan, K. *et al.* Correlates of protection against SARS-CoV-2 in rhesus macaques. *Nature* **590**, 630-634, doi:10.1038/s41586-020-03041-6 (2021).
46 Moss, P. The T cell immune response against SARS-CoV-2. *Nat Immunol* **23**, 186-193, doi:10.1038/s41590-021-01122-w (2022).
47 Sekine, T. *et al.* Robust T Cell Immunity in Convalescent Individuals with Asymptomatic or Mild COVID-19. *Cell* **183**, 158-168.e114, doi:https://doi.org/10.1016/j.cell.2020.08.017 (2020).
48 Lei, Y. *et al.* SARS-CoV-2 Spike Protein Impairs Endothelial Function via Downregulation of ACE 2. *Circ Res* **128**, 1323-1326, doi:10.1161/CIRCRESAHA.121.318902 (2021).
49 Olajide, O. A., Iwuanyanwu, V. U., Adegbola, O. D. & Al-Hindawi, A. A. SARS-CoV-2 Spike Glycoprotein S1 Induces Neuroinflammation in BV-2 Microglia. *Mol Neurobiol* **59**, 445-458, doi:10.1007/s12035-021-02593-6 (2022).

415 50 Shirato, K. & Kizaki, T. SARS-CoV-2 spike protein S1 subunit induces pro-inflammatory responses
416 via toll-like receptor 4 signaling in murine and human macrophages. *Heliyon* **7**, e06187,
417 doi:10.1016/j.heliyon.2021.e06187 (2021).

# 418 Materials and Methods

## 419 Cell culture and viruses

420 Vero E6 (CRL-1586) and M2-10B4 cells (ATCC CRL-1972) were cultured as described previously [26]. Caco-2
421 cells (ACC 169) were purchased from DSMZ (Braunschweig, Germany) and were cultured in DMEM (Gibco,
422 NY, USA) supplemented with 20% fetal bovine serum (FBS), 2 mM L-glutamine, 100 IU/mL penicillin and
423 100 µg/mL streptomycin. The FI strain of SARS-CoV-2 (GISAID database ID: EPI_ISL_463008) was described
424 previously as a D614G variant [51] and was passaged on Caco-2 cells in the biosafety level 3 (BSL3) laboratory
425 at HZI.

426 SARS-CoV-2 genome sequences are available on GISAID and GenBank under the following accession
427 numbers: SARS-CoV-2 B.1.351 (Beta) FFM-ZAF1/2021 (GenBank ID: MW822592) [52] and SARS-CoV-2
428 B.1.1.529 (BA.1) FFM-ZAF0396/2021 (EPI_ISL_6959868; GenBank ID: OL800703) [53]. $MCMV^{WT}$ refers to the
429 BAC-derived molecular clone (pSM3fr-MCK-2fl clone 3.3) [54]. $MCMV^{S}$ was generated by *en passant*
430 mutagenesis, as described previously [26]. Briefly, the codon-optimized S protein of the Wuhan variant
431 replaced the viral ie2 protein.

432 The expression vector for SARS-CoV-2 S protein of Omicron (BA.1) (based on isolate hCoV-
433 19/Botswana/R40B58_BHP_3321001245/2021; GISAID Accession ID: EPI_ISL_6640919) was generated by
434 Gibson assembly as described previously [55] and then subsequently introduced in pseudotype VSV
435 backbone that lacks VSV glycoprotein G (VSV-G) [56]. A plasmid encoding the S protein of SARS-CoV-2 Beta
436 (B.1.351) has been previously reported [26].

## 437 Virus stock generation and plaque assay

438 BAC-derived mutant MCMVs were propagated on M2-10B4 cells and concentrated by sucrose density
439 gradient centrifugation. BAC-derived MCMV was reconstituted by transfection of BAC DNA into NIH-3T3
440 cells (ATCC CRL-1658) using FuGENE HD transfection reagent (Promega, WI, USA) according to the
441 manufacturer's instructions. Transfected cells were cultured until viral plaques appeared and passaged 5
442 times in M2-10B4 cells before virus stock production. Virus stocks were prepared on ice. First,
443 supernatants of infected M2-10B4 cells were collected and infected cells were pelleted (5,000 × g for 15
444 min). The resulting cell pellets were homogenized in DMEM supplemented with 5% FBS and cell debris
445 was removed by centrifugation (12,000 x g for 10 min). Collected supernatants were resuspended in VSB
446 buffer (0.05 M Tris-HCl, 0.012 M KCl, and 0.005 M EDTA, adjusted to pH 7.8) and then concentrated by
447 centrifugation through a 15% sucrose cushion in VSB buffer (23,000 × g for 1.5 h). The resulting pellet was
448 re-suspended in 1-1.5 mL VSB buffer, briefly spun down, and supernatants were aliquoted and kept at -
449 80˚C.

450 SARS-CoV-2 D614G was generated and viruses were quantified by plaque assays as described before [26]
451 with a minor modification that Caco-2 cells were used for virus production. SARS-CoV-2 Beta and Omicron
452 BA.1 stocks were generated as described previously and titers were determined by the median tissue
453 culture infective dose ($TCID_{50}$) method [53].

454 Pseudotyped viruses were harvested as described before [26,55]. In brief, 293T cells were transfected with
455 expression plasmids (pCG1) encoding different S proteins of SARS-CoV-2 variants by using the calcium-
456 phosphate method. At 24h post-transfection, the medium was removed and cells were inoculated with a
457 replication-deficient VSV vector lacking its glycoprotein and coding instead for an enhanced green
458 fluorescent protein (GFP) (kindly provided by Gert Zimmer, Institute of Virology and Immunology,
459 Mittelhäusern, Switzerland). Following 1 h incubation at 37°C, the cells were washed with PBS, and culture
460 media containing anti-VSV-G antibody (culture supernatant from I1-hybridoma cells; ATCC CRL-2700)
461 were added. The pseudotype virus was harvested at 16-18 h post-infection.

## 462 Virus *in vivo* infection

463 K18-hACE2 mice were obtained from Jackson Laboratories and bred in the core animal facility of
464 Helmholtz Center for Infection Research, Braunschweig. BALB/c mice were purchased from Envigo (IN,
465 USA). All animals were housed under Specific Pathogen Free (SPF) conditions at HZI during breeding and
466 infection. All animal experiments were approved by the Lower Saxony State Office of Consumer Protection
467 and Food Safety.

468 K18-hACE2 mice (2-6 months old) were intraperitoneally (i.p.) immunized with $10^6$ PFU of recombinant
469 $MCMV^S$ or $MCMV^{WT}$ diluted in PBS or treated with PBS (200 µL per animal). BALB/c mice (4-7 months old)
470 were i.p. immunized with $2x10^5$ PFU of recombinant $MCMV^S$ or $MCMV^{WT}$. All mice were weekly or bi-
471 weekly monitored and scored for their health status after vaccination. Blood was analyzed at indicated
472 time points.

473 SARS-CoV-2 challenge experiments were performed in the HZI BSL3 laboratory essentially as described [57]
474 with the following modifications: K18-hACE2 mice were intranasally (i.n.) infected with $2x10^3$ PFU of
475 D614G SARS-CoV-2, while BALB/c mice were challenged with $6x10^4$ PFU of the VoCs. SARS-CoV-2-infected
476 mice were monitored for weight loss and clinical status daily, according to the animal permit.

477 SARS-CoV-2-challenged animals were scored daily to monitor any signs of disease development. Animals
478 were scored based on five criteria: spontaneous/social behavior, fur, fleeing behavior, posture, and
479 weight loss. Each score indicates the following: no signs of symptoms (score=0), mild and/or sporadic
480 symptoms (score=1), moderate and/or frequent symptoms (score=2), and severe symptoms with a clear
481 sign of heavy suffering (score=3). Weight loss criterion is scored as follows: ≤1 % (score=0), 1-10 %
482 (score=1), 10-20% (score=2), and >20% (score=3). Mice with a score of 3 in one criterion, or an overall
483 score of ≥9, were removed from the experiments.

## 484 Organ harvest

485 The trachea, lungs, heart, spleen, stomach, and brain were harvested at 3 or 7 days post-SARS-CoV-2
486 challenge, homogenized in 500 or 1,000 µL PBS with an MP Biomedical FastPrep 24 Tissue Homogenizer
487 (MP Biomedicals, CA, USA) and stored at -80°C until the usage for plaque assay or qRT-PCR analysis. In
488 animals that reached humane endpoints before 7 days post-challenge, organs were harvested on the day
489 of euthanasia.

## 490 RNA isolation and viral loads analyses

491 RNA was isolated according to the manufacturer's protocol (Rneasy RNA isolation kit, Qiagen). Shortly,
492 250 µL of organ homogenates in 750 µL Trizol were centrifuged at 16,000 x g for 3 min. The resulting
493 supernatants were carefully collected and washed with the same volume of 70% Ethanol. The mixed
494 solution was transferred into a collection tube and centrifuged at 10,000 x g for 30 sec. After decanting

495 the flow-through, the column was washed once with 700 µL of RW1 wash buffer and twice with 500 µL
496 RPE buffer. Lastly, 40 µL of nuclease-free water was added to the column for RNA elution, and isolated
497 RNAs were kept at -80°C.

498 Eluted RNAs were analyzed further to assess viral RNAs in the given organs by quantitative reverse
499 transcription polymerase chain reaction (RT-qPCR). The reaction was performed with a total volume of 20
500 µL containing 2 µL of sample RNAs or positive control RNAs, 5 µL TaqPath 1-step RT-qPCR Master Mix with
501 ROX reference dye, and 1.5 µL probe/primer sets. 2019-nCoV RUO kit was used to detect SARS-CoV-2
502 RNAs (Integrated DNA Technologies (IDT), USA), and Taqman Rodent GAPDH control reagents
503 (ThermoFischer Scientific, USA) were used for endogenous GAPDH RNAs. For absolute viral RNA
504 quantification, a standard curve was generated by serially diluting a SARS-CoV2 plasmid with the known
505 copy numbers 200,000 copies/µL (2019-nCoV_N_Positive Control, #10006625, IDT, USA) at 1:2 ratio in all
506 PCR analyses, with a quantitation limit of 20 copies of the plasmid standard in a single qPCR reaction. The
507 viral RNA of each sample was quantified in triplicate and the mean viral RNA was calculated by the
508 standard. RT-qPCR was performed using the StepOnePlus™ Real-Time PCR system (ThermoFischer
509 Scientific, USA) according to the manufacturer's instructions.

### 510 Detection of infectious SARS-CoV-2 in the lungs

511 Lung organ homogenates were serially diluted in DMEM (Gibco, NY, USA) supplemented with 5% FBS and
512 100 IU/mL penicillin, and 100 µg/mL streptomycin. 100 µL of sample dilutions were transferred onto
513 confluent VeroE6 cells in a 96-well format. After inoculation for 1 h at 37 °C, the inoculum was removed
514 and 1.5% methylcellulose in MEM supplemented with 5% FBS, 2 mM L-glutamine, 100 IU/mL penicillin,
515 and 100 µg/mL streptomycin was added to the cells. The infected cells were incubated at 37 °C for 48 h
516 before inactivation with a 4% formalin solution in PBS for 10 min at RT. The fixed cells were subjected to
517 immunofluorescent staining against the SARS-CoV-2 N protein. Briefly, fixed cells were permeabilized with
518 0.1% Triton X-100 (Sigma-Aldrich, MA, USA) for 10 min at RT and blocked with 1% BSA (Sigma-Aldrich, MA,
519 USA) in PBS for 30 min at RT. Thereupon, cells were incubated with a monoclonal anti-SARS-CoV-2 N
520 protein antibody (Abcalis, AB84-E02, 10 µg/mL) for 30 min at RT. After washing three times with PBS with
521 0.05% Tween-20 (PBS-T), a secondary antibody anti-mouse IgG conjugated with Alexa488 (Cell Signaling
522 Technology, #4408, 1:500) was added for 30 min at RT. After washing three times with PBS-T, the stained
523 cells were visualized using Incucyte S3 (Sartorius, Goettingen, Germany).

### 524 Flow cytometry quantification of S-specific T cells

525 Peripheral blood was harvested and red blood cells were removed by short osmotic shock. Thereupon,
526 lymphocytes were stained with S-derived VNFNFNGL-specific tetramers (Kindly provided by Ramon Arens,
527 Leiden University) for 30 min at RT. Subsequently, cells were stained with fluorescent-labeled antibodies
528 against CD3 (17A2, eBiosciences, CA, USA), CD4 (GK1.5, BioLegend, CA, USA), CD8a (53-6.7, BD Bioscience,
529 CA, USA), CD44 (IM7, BioLegend, CA, USA), CD11a (M17/4, BioLegend, CA, USA), CD62L (MEL-14,
530 BioLegend, CA, USA), and KLRG1 (2F1, BioLegend, CA, USA) for 30 min at 4°C. Dead cells identified by 7-
531 AAD viability staining solution (BioLegend, CA, USA) were excluded from all analyses. The labeled cells
532 were analyzed by flow cytometry (BD LSRFortessa™ Cell Analyzer) and subsequent analyses were done in
533 detail in FlowJo Software v10.

### 534 Detection of anti-spike antibodies in mouse sera

535 ELISA (Enzyme-Linked ImmunoSorbent Assay) was used to detect anti-S IgGs in vaccinated animal sera
536 and performed as described previously [58]. Briefly, antigens were immobilized on 384-well plates and

537 blocked with 2% milk powder in PBS-T. Mouse sera were serially diluted starting at a concentration of
538 1:100. S1-S2-His of different S variants were used to identify the antigen-specific binding and BSA or cell
539 lysates were used as control for unspecific binding. $EC_{50}$ was analyzed by a statistical analysis tool in
540 GraphPad Prism 9.

541 ### *In vitro* live virus neutralization titer (VNT) assay

542 The serum neutralization assay was performed as described before [26]. Briefly, heat-inactivated sera were
543 serially diluted and incubated with 100 PFU/100 µL of SARS-CoV-2 for an hour at RT. Thereupon, they
544 were transferred to 96-well plates seeded with Vero-E6 cells and inoculated with serum and virus for 1 h.
545 After the inoculum removal, the cells were overlaid with 1.5% methylcellulose and incubated at 37°C and
546 5% $CO_2$ for 3 days. The cells were fixed with 4% formaldehyde, followed by crystal violet staining and
547 plaque counting. Serum-neutralizing titer that results in a 50% reduction of virus plaques ($VNT_{50}$) was
548 analyzed by GraphPad Prism 9 nonlinear regression analysis.

549 ### Pseudovirus neutralization assay

550 Pseudovirus neutralization assays were performed as described in the previous publications [4,26]. For
551 neutralization experiments, pseudotyped particles and heat-inactivated serum dilution were mixed at a
552 1:1 ratio and incubated for 60 min at 37°C before being inoculated onto VeroE6 cells grown in 96-well
553 plates. At 24 h post-infection, GFP expression was measured by using Incucyte S3 (Sartorius, Goettingen,
554 Germany).

555 ### Statistics

556 One-way ANOVA with Kruskal-Wallis correction was performed for multiple-group analysis. Two-tailed
557 Mann-Whitney tests were used to compare the difference between two independent groups. Log-rank
558 (Mantel-cox) tests were performed to compare the survival distributions of groups. Statistical analysis was
559 calculated by GraphPad Prism 9.

560 ### Data availability

561 All SARS-CoV-2 genome sequences are available as mentioned above. The D614 SARS-CoV-2 variant
562 (GISAID database ID: EPI_ISL_463008), SARS-CoV-2 B.1.351 (Beta) FFM-ZAF1/2021 (GenBank ID:
563 MW822592), and SARS-CoV-2 B.1.1.529 (BA.1) FFM-ZAF0396/2021 (EPI_ISL_6959868; GenBank ID:
564 OL800703).

565 ## Materials and Methods reference

566 51 Chaudhry, M. Z. *et al.* Rapid SARS-CoV-2 Adaptation to Available Cellular Proteases. *J Virol* **96**,
567 e0218621, doi:10.1128/jvi.02186-21 (2022).

568 52 Widera, M. *et al.* Limited Neutralization of Authentic Severe Acute Respiratory Syndrome
569 Coronavirus 2 Variants Carrying E484K In Vitro. *The Journal of infectious diseases* **224**, 1109-1114,
570 doi:10.1093/infdis/jiab355 (2021).

571 53 Wilhelm, A. *et al.* Limited neutralisation of the SARS-CoV-2 Omicron subvariants BA.1 and BA.2
572 by convalescent and vaccine serum and monoclonal antibodies. *EBioMedicine* **82**, 104158,
573 doi:10.1016/j.ebiom.2022.104158 (2022).

54 Jordan, S. *et al.* Virus progeny of murine cytomegalovirus bacterial artificial chromosome pSM3fr show reduced growth in salivary Glands due to a fixed mutation of MCK-2. *J Virol* **85**, 10346-10353, doi:10.1128/JVI.00545-11 (2011).

55 Hoffmann, M. *et al.* SARS-CoV-2 Cell Entry Depends on ACE2 and TMPRSS2 and Is Blocked by a Clinically Proven Protease Inhibitor. *Cell* **181**, 271-280 e278, doi:10.1016/j.cell.2020.02.052 (2020).

56 Hoffmann, M. *et al.* The Omicron variant is highly resistant against antibody-mediated neutralization: Implications for control of the COVID-19 pandemic. *Cell* **185**, 447-456.e411, doi:10.1016/j.cell.2021.12.032 (2022).

57 Bertoglio, F. *et al.* A SARS-CoV-2 neutralizing antibody selected from COVID-19 patients binds to the ACE2-RBD interface and is tolerant to most known RBD mutations. *Cell Rep* **36**, 109433, doi:10.1016/j.celrep.2021.109433 (2021).

58 Bertoglio, F. *et al.* SARS-CoV-2 neutralizing human recombinant antibodies selected from pre-pandemic healthy donors binding at RBD-ACE2 interface. *Nat Commun* **12**, 1577, doi:10.1038/s41467-021-21609-2 (2021).

## Acknowledgment

We thank Inge Hollatz-Rangosch for her technical assistance. We acknowledge colleagues from HZI for their professional expertise, Lothar Gröbe from the flow cytometry facility, Susanne Talay from the S3 facility, Marina Pils, Katrin Schlarmann, Petra Beyer, and Bastian Pasche from the animal facility, and Katarzyna M. Sitnik and Natascha Goedecke for support with animal ethical issues. We express our gratitude to Stipan Jonjic and Astrid Krmpotic for the scientific discussion. This research was supported by the grant 14-76103-84 from the Ministry of Science and Culture of Lower Saxony and by the EU Partnering grant MCMVaccine (PEI-008) from the Impulse and Networking Fund of the Helmholtz Association to LCS and SP.

## Author Contributions

Y.K. and L.C.S. conceived and designed the study; Y.K. H.J. and B.F. performed *in vivo* experiments; F.B. and M.Hu. performed and analyzed ELISA serology; Y.K., H.J., and F.B. analyzed the data; Y.K. and L.C.S. interpreted the data; Y.K. and L.C.S. wrote the manuscript; K.E., M.Z.C., M.W., S.C., M.Ho., and S.P. provided recombinant virus or clinical isolates; L.C.S. supervised the study.
All authors reviewed the results and approved the final version of the manuscript. Correspondence and requests for materials should be addressed to L.C.S.

## Competing interests

The authors LCS and YK are applicants for a patent based on MCMV as a vaccine vector. The authors declare no other competing interests.